

promoting access to White Rose research papers



Universities of Leeds, Sheffield and York
<http://eprints.whiterose.ac.uk/>

This is an author produced version of a paper published in ***Computers & Fluids***
White Rose Research Online URL for this paper:
<http://eprints.whiterose.ac.uk/11155>

Published paper

Barber, S., Chin, S.B., and Carré, M.J. Sports ball aerodynamics: A numerical study of the erratic motion of soccer balls. *Computers and Fluids*, 38, 6 (2009), 1091-1100.

<http://dx.doi.org/10.1016/j.compfluid.2008.11.001>

Sports ball aerodynamics: a numerical study of the erratic motion of soccer balls

S. Barber, S.B. Chin and M.J. Carré

Department of Mechanical Engineering, University of Sheffield, S1 3JD, UK

+44(0)1142227839

barbers@ethz.ch, s.b.chin@shef.ac.uk, m.j.carre@shef.ac.uk

The application of the commercial CFD code, FLUENT, to sports ball aerodynamics was assessed and a validated 3D analysis technique was established for balls that have been scanned with a 3D laser scanner or drawn in CAD. The technique was used to examine the effects of surface geometry on the aerodynamic behaviour of soccer balls by comparing the flow around different balls and predicting the aerodynamic force coefficients. The validation process included performing CFD studies on 3D smooth spheres and various soccer balls, and comparing the results to wind tunnel tests and flow visualisation. The CFD technique used a surface wrapping meshing method and the Reynolds-Averaged Navier-Stokes approach with the realizable $k-\varepsilon$ turbulence model, which was found to be able to predict the drag, lift and side force coefficients (C_D , C_L and C_S) reliably, to compare the wake behaviour, and to give good pressure distributions near the stagnation point. The main limitations of the technique with the available computational resources were its inability to accurately predict boundary layer transition or growth, but despite this, several conclusions could be drawn regarding soccer ball aerodynamics. C_D was not significantly different between balls. C_L and C_S were found to be significantly affected by the orientation of the ball relative to its direction of travel, meaning that balls kicked with low amounts of spin could experience quasi-steady lift and side forces and move erratically from side-to-side or up and down through the air. For different balls, C_D , C_L and C_S were predicted and their variation with orientation entered into a modified trajectory simulation program. The erratic nature of this type of kick was found to vary with details of the surface geometry including seam size, panel symmetry, number, frequency and pattern, as well as the velocity and spin applied to the ball by the player. Exploitation of this phenomenon by players and ball designers could have a significant impact on the game.

Keywords: Football, soccer, CFD, aerodynamics, drag, sports balls

Nomenclature

$Re = \frac{\rho v d}{\mu}$	Reynolds number	
$Sp = \frac{r\omega}{v}$	Spin parameter	
$C_D = \frac{D}{1/2 \rho v^2 A}$	Drag coefficient	
C_L	Lift coefficient	
C_S	Side force coefficient	
v	Velocity	[m/s]
d	Ball diameter	[m]
r	Ball radius	[m]
ρ	Density	[kg/m ³]
A	Ball cross-sectional area	[m ²]
D	Drag force	[N]
μ	Dynamic viscosity	[Pa s]
y^+	y plus value	
ω	Spin rate	[rad/s]

1. Introduction

1.1 Background

The flight of a ball through the air is a key part of many popular sports, and gaining an understanding of the aerodynamics can help equipment designers, players, coaches and game regulators and make the game more interesting for the fans. Soccer is widely regarded as the most popular sport in the world, and the exact speed, swerve or dip of a soccer ball can be match-deciding. Recent developments in soccer ball manufacturing technologies have led to the possibility of radical changes in surface geometry and seam configurations, and the consequences of such changes can only be fully predicted if the aerodynamic behaviour is understood.

A number of wind tunnel tests, flow visualisation and numerical studies have been undertaken on both smooth and rough non-spinning spheres at a high Re relevant to soccer balls. These include drag coefficient (C_D) measurements by Achenbach [1, 2], wake flow visualisation with smoke and tufts in a wind tunnel by Taneda [3], and RANS and LES computations by Jindal *et al.* [4] and Constantinescu *et al.* [5]. The behaviour of smooth spheres at high Re is well-documented.

However, relatively few CFD studies have been undertaken on sports balls due to the required computational power, difficulty of meshing and perhaps a previous lack of demand for a highly detailed understanding. 3D qualitative CFD analysis was carried out on a non-spinning cricket ball for both laminar and turbulent flow (using ANSYS FLOTRAN with the standard $k-\varepsilon$ turbulence model) by Penrose *et al.* [6] and on a rotating baseball (using an in-house code for the laminar regime only) by Himeno [7].

Various CFD studies on spinning golf balls have been carried out using FLUENT. One set of studies by Ting [8-10] used a rather small flow domain (dimensions of $0.254 \times 0.2032 \times 0.2032$ m and only approximately 1.63×10^5 unstructured tetrahedral cells) and the Spalart-Allmaras turbulence model, which showed reasonable C_D agreement for laminar solutions and allowed qualitative wake structure comparisons to be made for turbulent solutions for spinning balls; another by Aoki *et al.* [11] produced results that were only over-predicted by approximately 5% when compared to experimental data (using LES with a grid that had dimensions $0.76 \times 0.76 \times 1.38$ m and contained about 1 million unstructured cells in total). Additionally, simulation of the 3D flow around dimpled cylinders by Kim *et al.* [12] predicted a reasonable C_D for lower Reynolds number, Re , (getting towards transition) but too high for higher Re (using an in-house code with the Spalart-Allmaras turbulence model on a grid that contained approximately 2.4 million tetrahedral and prism elements).

There is no consensus yet as to the most appropriate CFD technique for modelling sports ball aerodynamics, therefore this work covered a thorough consideration of the available meshing and modelling techniques.

1.2 Aims

The aims of this study were to assess the use of FLUENT as a tool for modelling the aerodynamic behaviour of sports balls (within the limits provided by the computational resources available), to establish a validated 3D technique for the analysis of soccer balls in FLUENT, and then to use the technique to help understand the aerodynamics of soccer balls and the effects of surface geometry on their trajectories.

1.3 Resources and limitations

The commercially-available CFD software, FLUENT Version 6.2, and its pre-processing components, GAMBIT and TGRID4, were available for use in this study. The computational resources available to the study meant that, in practical terms, grid sizes were limited to approximately 9 million cells, but at this size they were slow to produce, manipulate and transfer, and file storage space was limited. Solutions typically took 2-4 days to reach full convergence using the steady-state RANS equations (parallel processing, shared server).

These limitations required the assumption of a fully turbulent boundary layer. In a previous study, Barber *et al.* [13] found that laminar to turbulent transition occurs at $Re \approx 2.0 \times 10^5 - 3.0 \times 10^5$ for soccer balls, corresponding to $v \approx 11-20$ m/s. The type of free-kick studied in this work is the low-spin, high-velocity kick that is generally launched at a velocity of 30-35 m/s, which is well into the turbulent flow regime. An in-house trajectory simulation programme developed by Carré *et al.* [14] showed that a ball launched at this velocity slows to approximately 21 m/s by the end of its flight, which is still in the turbulent regime. Hence it was deemed valid for this study to assume that the flow was always fully turbulent.

The computational limitations required the use of the steady-state Reynolds Averages Navier-Stokes (RANS) approach. It was thought that over the range of Re experienced by the flow around a football ($\sim 10^6$), unsteady effects would be of secondary importance, and hence the aerodynamic coefficients would be largely unaffected by this and a steady state flow analysis would provide useful information at relatively low computational cost.

Additionally, the constraints required the use of a hybrid meshing technique and the study of non-spinning balls only.

2. Validation

A large part of this study involved the validation procedure, which is given in detail by Barber [15]. Studies were undertaken in order to become familiar with the FLUENT software and with the physics of the flow, and to assess the use of FLUENT as a tool for analysing sports ball aerodynamics. The geometry was made progressively more complex, and solutions were continuously compared to experimental results for validation purposes. The studies included a 3D smooth sphere, the CAD geometry of a scale model soccer ball and a scanned soccer ball. The study culminated in the production of a preferred CFD methodology for the 3D analysis of soccer ball aerodynamics in FLUENT, which uses the realizable $k-\varepsilon$ turbulence model, a surface wrapping meshing technique and a hybrid mesh mainly consisting of 3D structured hexahedral elements with a near-wall cell size of 0.01 mm.

2.1 Mesh design

For each study, the following aspects were taken into consideration:

Domain size: The domain must be large enough to ensure that its outer surfaces have minimal effect on the flow. Placing the surface of the ball, diameter d , at $5d$ from the inlet, $20d$ from the outlet and $5d$ from the sides of the domain was found to be sufficient.

Near-wall cell size: The required size of the first cell at the surface of the ball was dictated by the chosen method of modelling near the wall. For the soccer balls, enhanced wall treatment was used, and to obtain sufficient accuracy to model the boundary layer and resolve the viscous sub-layer, y^+ was required to be approximately equal to 1 (y^+ represents a non-dimensional wall distance that is used to define different sections of a boundary layer).

Cell skewness: Cell skewness is a measure of grid quality, and is measured between 0 and 1, where skewness = 0 indicates an equiangular cell, 0-0.25 is excellent, 0.25-0.5 is good, 0.5-0.75 is fair, 0.75-0.9 is poor, 0.9-1 is very poor and 1 is degenerate. According to the FLUENT user guide [16] a general guide is to try and keep the skewness of all cells below 0.75.

Cell aspect ratio: Cell aspect ratio is another measure of grid quality, and a general rule-of-thumb specified in the FLUENT user guide is to keep the aspect ratio of all the cells in the grid below 5; however it is said to be acceptable for the value to reach 10 in regions aligned with the flow.

Boundary conditions: For each case, the outlet was specified as an outflow, and the inlet defined by the fluid velocity. The surface of the geometry was defined as a no-slip wall, and the far field boundaries of the solution domain were defined as a slip-wall, i.e., a wall with zero shear stress.

To alter Re over the required range, the velocity was altered between 10 and 30 m/s and the fluid viscosity was altered between 1.6691×10^{-5} and 5.3410×10^{-6} kg/ms, which was necessary to keep y^+ down as the velocity increased. Density was kept constant at 1.225 kg/m^3 . The turbulence intensity (the ratio of the root-mean-square of the velocity fluctuations to the mean flow velocity) and length scale (a physical quantity related to the size of the large eddies that contain the energy in turbulent flows, defined as $0.07 \times \text{duct width}$ [16]) at the inlet were set to 0.1% and 0.07 m, respectively, to match the wind tunnel conditions for comparison purposes. The exact value of turbulence intensity was initially varied from about 10% to 0.1%, and appeared to have very little effect on the results. Convergence was monitored with strict residual criteria of 10^{-5} and force coefficient monitoring.

For each study, C_D was predicted at a range of Re in the super- and trans-critical regimes, and details of the flow were compared to those of corresponding experimental results. Only the highest Re tested was expected to correspond to a fully-turbulent boundary layer – the lower simulations were undertaken in order to observe trends and Re -dependency.

2.2 Summary of validation

For each type of geometry that was analysed, a grid dependency study and a turbulence model study was undertaken. The procedure is summarised here.

The drag results were compared to wind tunnel force measurements and the wake structure to experimental flow visualisation. The basic mesh structure, containing structured 3D quadrilateral cells, was the same for every study and is illustrated in Figure 1. A table summarizing the C_D results compared to experiment for each study

and turbulence model is shown in Table 1. These ranges are very high due to the general difficulties of separation point prediction in the RANS approach and the very high sensitivity of C_D on the separation position. The most suitable turbulence model for each application is highlighted with a star in the table. The optimum solver details for each case are summarised in Table 2.

Experimental C_D vs. Re results for a smooth sphere and various soccer balls (pictured in Figure 2) are shown in Figure 3. In general, a large drop in C_D is seen at a certain Re , when the boundary layer transitions from laminar to turbulent flow. C_D reaches a minimum (C_{Dmin}) at the critical Reynolds number (Re_{crit}), when turbulent boundary layer separation first occurs. As Re is increased beyond Re_{crit} , transition takes place earlier on the surface, and C_D rises as the skin friction drag increases.

FLUENT was found to be capable of predicting average wake structures that compared well with wind tunnel flow visualisation for the 3D smooth sphere, the scale model soccer ball and the real soccer ball. However, several discrepancies were found between the CFD results and the wind tunnel results, and in general the following applied:

- The expected drop in C_D in the critical regime could not be predicted because boundary layer transition could not be modelled;
- The rise in C_D in the super-critical regime could not be modelled for a combination of reasons: the boundary layer was modelled as fully turbulent whereas in reality it is a combination of laminar and turbulent in the super-critical regime, and in some cases FLUENT switched from near-wall modelling to the

standard wall function at high Re (because a range of Re were studied and computational constraints prevented y^+ from staying ≈ 1 at the higher Re), not fully resolving the boundary layer and affecting separation;

- The C_D values were generally lower than experiment because the effects of the flow interaction between the sphere and its supporting device could not fully taken into consideration (implying that the experimental results are indeed slightly higher than reality – see the study in Barber [13] for more details);
- Convergence was difficult to reach and wake asymmetries suggested large numerical errors for all the turbulence models except for the standard $k-\varepsilon$ and realizable $k-\varepsilon$ models – this is due to the over-prediction of turbulent kinetic energy of the $k-\varepsilon$ models (which reduces the accuracy of the prediction of separation);
- Even though a mesh dependency study was carried out, inaccuracies could result from the tetrahedron-to-quadrilateral transition region and the hanging-node formulation further out.

The analyses were limited by computational power and software availability, and FLUENT was found to be a difficult tool for this application. The meshing process was very time-consuming and convergence for a real soccer ball was only achieved after altering the numerical model parameters. Despite these problems, the results suggest that FLUENT can be used as an effective tool for comparison between different ball designs.

The most suitable and accurate meshing and solving techniques that were chosen for the analysis of soccer balls were combined together into an analysis tool, which used

the solving parameters shown in Tables 1 and 2 for the real soccer balls, along with a mesh structure as shown in Figure 4. The mesh varied slightly between balls, but in general had about 9 million cells with prism cells growing from the surface and a section of unstructured tetrahedral cells joining them to the outer structured mesh. Once imported into TGRID4, the scanned geometry of a ball was immediately converted to a surface mesh using a new wrapping tool.

The use of the analysis tool to compare the behaviour of several different soccer balls is discussed below.

3. Soccer ball analysis

3.1 Scanned balls

3.1.1 Set-up

Scanned geometries of seven different balls (Balls 1-7) were entered into FLUENT, which was set up as described in the previous section. Studies were undertaken at various ball orientations about the vertical y -axis (rotated at 10° intervals from 0° to 90°) at $Re = 1.0 \times 10^6$. This was done by importing the scanned geometry into GAMBIT, rotating the geometry manually to 0° and then using the rotating tool in GAMBIT to move the geometry to the other orientations. 0° was defined for each ball as illustrated in Figure 2. Different orientations were studied in order to analyse the behaviour of balls launched with very low amounts of spin. For the orientations of 0° , the study was repeated for $Re = 1.6 \times 10^5$ and 6.0×10^5 in order to examine Re -dependency effects.

Ball 1 had 32 panels (20 pentagonal and 12 hexagonal) that were hand-stitched together in the traditional manner. Ball 2 had 32 panels that were thermally bonded together, and hence had narrower, shallower and sharper seams. Ball 3 had 14 pre-curved panels that were thermally bonded together. Balls 4-7 were similar to a standard 32 panel ball, but some of the panels were joined together. The four balls varied in arrangement and alignment of the panels and they were generally not rotationally symmetrical at an orientation of 0° . Ball 4 and Ball 5 had 12 additional joins between hexagons and pentagons making a total of 20 panels, but were different in the way the panels are joined. Ball 6 and Ball 7 had 6 additional joins between

hexagons making a total of 26 panels, and were oriented slightly differently to each other. The resolution of the mesh was such that each seam contained at least 10 grid points.

3.1.2 Drag results

The C_D results for Balls 1-3 are shown in Figure 3 and compared to known data of Achenbach [1] and Barber *et al.* [15]. The results for Balls 4-7 were very similar and are therefore not shown. C_D was higher for each ball than for the smooth sphere, and lower than the wind tunnel results for the scale model soccer ball, due to the relative seam sizes.

As shown in Figure 3, C_D for Ball 3 was under-predicted compared to the wind tunnel results (by about 3-5% in the super-critical regime and about 25% in the trans-critical regime). The reasons for this were because the flow was modelled as fully turbulent for the entire Re range, and the effects of the flow interaction between the ball and its supporting device were not deducted from the wind tunnel C_D values. The C_D values were split into skin friction and pressure drag components, and the skin friction drag was approximately 0.030-0.035 for the lowest Re and 0.020-0.025 for the highest Re (depending on the ball).

C_D for Ball 2 was approximately 15% larger than for Ball 1 possibly due to slightly earlier separation caused by the sharper seams. C_D for Ball 3 was approximately 6% smaller than for Ball 1 due to a decrease in both pressure and skin friction drag with the smaller and fewer seams. These trends matched the wind tunnel results around the super-critical regime [15]. Flow visualisation (velocity contours taken at a central plane, side view and total pressure contours on the surface) for the three balls and the

smooth sphere at $Re = 1.0 \times 10^6$ is shown in Figure 5. The wakes were all similar in size, explaining the fairly similar C_D values seen, and compared well with experimental flow visualisation of Asai [17].

Additionally, the wakes appear slightly asymmetric and possibly unsteady. Even though unsteady effects were expected not to be significant, it is recommended that further work is carried out to investigate this effect in more detail. This could also take into account the oscillation of the ball following deformation after it is kicked, even though this effect is generally assumed to be small. This is not, however, within the scope or the computational constraints of the present work.

3.1.3 Variation with orientation

Force coefficients

In general, C_L and C_S were found to vary with orientation due to the asymmetry of the scanned geometry, but C_D remained constant. The predicted variations of C_S for Balls 1-3 are shown in Figure 6. For Balls 1-3, C_L did not vary significantly due to symmetry about the perpendicular axis so are not included.

Position of separation

These variations can be explained by considering how the position of separation relates to the surface geometry of the balls. The same argument could also partly explain the under-prediction of C_D described earlier.

Figure 7 shows the simulated oil flow visualisation (from four different views) around Ball 1 at 0° for $Re = 1.0 \times 10^6$, demonstrating the pathlines of particles released from the surface and showing clearly the separation position towards the rear of the ball.

Each particle had its own “particle ID” and the particles were coloured according to their ID. For each ball, images were then built up that indicated the position of separation at all points around the ball, and the influence of the seams were seen. Figure 8 shows shear stress contours (Pa) on the rear surface of Balls 1-3, along with approximate separation points obtained from the oil flow visualisation. Black lines indicate approximate separation and red lines indicate separation where the flow is particularly affected by the presence of a seam.

The images in Figure 8 suggest that seams that are perpendicular, or nearly perpendicular, to the flow had an effect on the position of separation, due to the sudden change in curvature of the surface. The less perpendicular to the flow a seam was (i.e. the more aligned with the flow) the more likely the flow was to continue in its original direction and not be affected largely by the seam. In general, the seams of Ball 1 that were perpendicular (or nearly perpendicular) to the flow seem to have been more likely to hold back the flow and alter its position of separation than the seams of Ball 2, probably because they were larger and had more influence on the flow (e.g. Ball 1 compared to Ball 2 at 20° and 30°). This meant that the C_S varied more often with angle for Ball 1. The seams of Ball 3 only rarely held back the flow and influenced separation, but was sometimes swayed heavily by the presence of long, perpendicular seams, e.g. at 40° and 50° (Figure 8). The magnitude of C_S was correspondingly lower for Ball 3.

The significant “stepped” pattern in C_S occurred when particular seams held back the flow in a certain position, and continued to do so as the ball was rotated. Eventually it reached a point where the seam suddenly lost its influence because it was too far away

from the natural position of separation (i.e. where separation would have occurred without the presence of the seams), and the separation point then retreated to the previous perpendicular seam. This was particularly evident between 50° and 80° for Ball 1. The pattern occurred less frequently for Ball 2 because a seam was less likely to hold back the flow near separation and remain holding it back as the ball rotated. The large drop in C_S from 50° to 60° is explained by a sudden jump in separation on one side of the ball. The variation in C_S was less for Ball 3 in general; however the occasional sudden peak was seen. The peak at 40° was explained by the strong bias of the flow to separate near the long, vertical seam on one side. At 50° the separation region jumped back to the previous vertical seam.

Further considerations

As well as altering the positions of separation, the asymmetrical surface geometry resulted in corresponding asymmetric wakes, an example of which is given in Figure 9. It should be noted that these wakes could decrease the stability and result in further convergence problems for turbulence models other than the $k-\varepsilon$ models.

Another factor that could be connected to this effect was thought to be the roundness of the balls. The geometries of Ball 1 and Ball 3 were examined in more detail using radius contour plots in FLUENT. The plots are shown in Figure 10, in which contours of radius are displayed at a range that captures the surface of the balls. If the balls were completely round, the seams consistent, and the reference point (0,0) perfectly in the centre of the ball, then the panels would all be red and the seams would be blue. However, the ball geometries were clearly not perfectly round, and the radius range for the panels of Ball 1 was approximately 0.108-0.110m and approximately 0.108-

0.111 m for the panels of Ball 3. This 2-3 mm discrepancy could have been caused by a number of factors, including manufacturing inconsistencies, scanning errors, surfacing errors (resulting from the approximations made when holes were filled in the scanned geometry to produce the surface) or errors in defining the centre of the ball in the software. It could contribute to the asymmetry of the balls and thus contribute to the varying C_L values. However, it was not possible to separate these effects from those thought to be caused by the seams.

For Balls 4-7, similar analysis showed that the seam positions near separation seemed to have an effect on the flow, because they directly affected the position of separation. The results suggested that the exact positioning of the balls in the mesh had as much effect on the flow as their seam arrangement and hence the trajectories were thought to be very sensitive to orientation. It was thought that the variations of C_S for Balls 4-7 were less defined than for Balls 1-3 because they had fewer seams.

Validation

Ideally these findings should be confirmed through controlled experiments, but wind tunnel tests that accurately measure C_L and C_S have not yet been done. However, trajectory analysis does show that the magnitude and frequency of the values obtained in this study would result in similar trajectories to those observed in reality. This is discussed below and in more detail in Barber [15].

3.1.4 Effects on trajectory

Balls launched with high velocity and low spin (< 2 rev/s) are often seen to “move in the air” during their flight and behave erratically, as opposed to spinning balls that swerve in the air due to the Magnus effect in a predictable manner.

In order to examine whether this effect could be attributed to the observed effects discussed in this study, a fully-validated trajectory simulation programme was used. The variations in C_L and C_S were entered into the programme for a kick similar to one observed in the English Premiership in 2006, shown approximately in Figure 11. The kick was taken at 33 m from goal, slightly to the right of centre, launched at approximately 36 m/s with $\frac{1}{4}$ rev/s of sidespin.

The resulting trajectory showed similar behaviour to those observed in reality, as the example in Figure 12 for Balls 1, 2 and 3 for an initial orientation of 0° verifies. The effects of a change in initial orientation and ball type on the resulting trajectory were investigated. The analysis of the results (given in more detail in Barber [15]), brought up the following factors that appear to affect the trajectory of a ball launched with low amounts of spin:

- **Number of seams:** more seams (especially ones that are perpendicular to the flow near separation) increase the maximum force coefficient, which would increase the amount of swerve, which may or may not lead to a less consistent range (depending on the frequency of force coefficient variation, spin rate and initial orientation);
- **Depth of seams:** deep seams increase the maximum force coefficient, which would increase the amount of swerve;
- **Symmetry of pattern in a given direction:** the less symmetry about an axis, the larger the force coefficient is perpendicular to that axis and the flow direction,

increasing the amount of swerve; if the pattern is symmetrical, the force coefficient would be zero perpendicular to the axes of symmetry;

- **Frequency of repeating pattern in flow direction:** a lower frequency pattern (i.e. larger panels in the flow direction) reduces the frequency of the force variation, which would reduce the number of swerves during flight and could make the flight less consistent (depending on the spin rate and the initial orientation).

The most consistent balls are the ones that have the optimum combination of maximum force coefficient and frequency relative to the amount of applied spin.

These observations hold as long as the behaviour remains pseudo-static and the spin rate remains low enough so that the Magnus Effect does not take over. This is expected when the Magnus coefficient (C_M) exceeds the pseudo-static force coefficient, at $Sp \approx 0.1$ ($\omega \approx 2$ rev/s at 30 m/s), taken from the C_M vs. Sp graph in Carré [9].

3.2 Uncertainty analysis

Even though validation studies were done throughout the work, the effect of the unstructured region of the mesh was not known. It was thought that uncertainties could arise from the fact that this part of the mesh was different for each ball and orientation (because it had to be re-made each time). Other possible sources of uncertainty included manufacturing inconsistencies of the balls, scanning and surfacing inconsistencies and alignment inconsistencies when the balls were oriented at 0° by eye.

These uncertainties were analysed by undertaking further studies on a smooth sphere, a repeatability study on Ball 3 and an alignment study on Ball 1, all of which are described in detail by Barber [15]. The conclusions of this study are discussed here.

The CFD analysis methodology that was developed was found to predict the flow structure around a smooth sphere well, with a wake structure similar to that of wind tunnel flow visualisation. It under-predicted C_D (by approximately 0.08) at very high Re ($Re > 1.0 \times 10^6$) and C_L and C_S values were close to zero (approximately 0.01). The addition of a section of unstructured mesh around the sphere (combining the use of the PRESTO! pressure discretisation scheme and the PISO pressure-velocity coupling) improved the speed of convergence and resulted in a more accurate prediction of the wake.

The inherent error in the calculation of C_L and C_S in the CFD process due to the mesh was found to be 0.01. Additionally, a 2-3 mm discrepancy in the diameter was found for the balls due to inconsistencies in manufacturing, scanning and surfacing processes. Repeat scans could alter the force coefficient variation curves by a maximum of ± 0.02 , due to inconsistencies in the geometry, in the unstructured region of the mesh and in the manual alignment of the geometry in the mesh by eye. It was found that a $\pm 2^\circ$ alteration of the geometry around its 0° position could not be easily detected by eye, and variations of $\pm 2^\circ$ in a ball's geometry due to misalignment could alter the force coefficients by approximately ± 0.02 . It was concluded that the same type of balls launched with low amounts of spin will not behave consistently from ball

to ball because the flight depends on their geometry and roundness as well as on the angle of orientation.

3.3 Evaluation of FLUENT

3.3.1 Practicalities

The main limitations of the use of FLUENT for this application were due to the availability of computational power, as discussed in Section 1.3. FLUENT also had a number of practical limitations, for example it was especially difficult to design the structured part of the mesh and the desired results were difficult to obtain from the y^+ adaption tool. Convergence was difficult to achieve for this application, and could only be achieved for the realizable $k-\varepsilon$ model after altering the numerical model parameters. The $k-\varepsilon$ models over-predict the turbulent kinetic energy and stabilise the solutions enough for convergence. As discussed in Section 2.2, the accuracy of the solutions is therefore compromised.

3.3.2 Uncertainties

In the validation studies, FLUENT was found to be capable of predicting average wake structures that compared well with wind tunnel flow visualisation for a soccer ball, and, despite some limitations, it was found to be an effective tool for qualitative (or perhaps relative) comparison between different ball designs.

The main limitations were that boundary layer transition could not be predicted, unsteady effects were not modelled and FLUENT was not capable of modelling boundary layer thickening. This resulted in under-predictions of C_D up to 50% for the

smooth sphere, 20% for the scale model ball and 25% for the real soccer ball at the highest Re (1.0×10^6).

Small asymmetries due to inconsistencies in manufacturing, scanning, surfacing, geometry alignment and in the unstructured part of the mesh introduced some uncertainties into the analysis, and repeat scans were found to alter the force coefficient variation curves by a maximum of ± 0.02 .

4. Conclusions

The CFD analysis tool was found to be a powerful tool for the comparative analysis of soccer ball aerodynamics, even though there were some limitations with the software capabilities and the available computational resources.

Several different scanned and altered soccer balls were analysed using FLUENT. C_D was not significantly different between different ball designs. Both C_L and C_S were found to vary significantly with orientation and with ball type due to asymmetrical geometry causing variation in separation around the seams. When these quasi-steady variations for each ball were approximated and then entered into the trajectory simulation programme, each ball was found to behave quite differently, and erratic trajectories were observed for spin rates < 2 rev/s.

The analysis allowed some general conclusions to be drawn regarding the effects of ball surface geometry on its trajectory. **More seams** (especially ones that are perpendicular to the flow near separation) increase the maximum force coefficient, which would increase the amount of swerve for low-spinning kicks, which may or

may not lead to a less consistent range (depending on the frequency of force coefficient variation, spin rate and initial orientation). **Deep seams** increase the maximum force coefficient, which would increase the amount of swerve. **The lower the symmetry of the surface pattern about an axis**, the larger the force coefficient is perpendicular to that axis and the flow direction, increasing the amount of swerve; if the pattern was symmetrical, the force coefficient would be zero perpendicular to the axes of symmetry. **A lower frequency of repeating surface pattern** (i.e. larger panels in the flow direction) reduces the frequency of the force variation, which would reduce the number of swerves during flight and could make the flight less consistent (depending on the spin rate and the initial orientation).

The most consistent balls are the ones that have the optimum combination of amplitude and frequency of the varying force coefficient relative to the amount of applied spin.

Acknowledgements

Thanks to Fluent Europe and the EPSRC for supporting this study, and to Richard Lukes, John Hart and Dave Mann for their technical advice and support.

References

1. Achenbach E, *Experiments on the flow past spheres at very high Reynolds numbers*. Journal of Fluid Mechanics, 1972. **54**: p. 565-575.
2. Achenbach E, *The effects of surface roughness and tunnel blockages on the flow past spheres*. Journal of Fluid Mechanics, 1974. **65**: p. 113-125.
3. Taneda S, *Visual observations on the flow past spheres at Reynolds numbers between 10^4 and 10^6* . Journal of Fluid Mechanics, 1978. **85**: p. 187-192.
4. Jindal S, Long LN, Plassmann PE, and Sezer-Uzol N, *Large-eddy simulations around a sphere using unstructured grids*. AIAA Paper 2228.
5. Constantinescu GS, Chapelet M, and Squires KS, *Turbulence modelling applied to flow over a sphere*. AIAA Journal, 2003. **41** (9): p. 1733-1743.
6. Penrose JMT, Hose DR, and Trowbridge EA. *Cricket ball swing: a preliminary analysis using CFD*. in The Engineering of Sport. 1996. Sheffield, UK: AA Balkema.
7. Himeno R, *Computational study of influences of a seam line of a ball for baseball on flows*. Journal of Flow Visualisation, 2001. **4**: p. 197.
8. Ting LL. *Application of CFD technology analysing the 3D aerodynamic behaviour of dimpled golf balls*. in ASME International Mechanical Engineering Congress and Exposition. 2002. New Orleans, Louisiana, USA.
9. Ting LL. *Effect of teardrop shaped dimple design on the golf ball aerodynamic performance*. in ISEA 5th Engineering of Sport Conference. 2004. Davis, California: International Sports Engineering Association.
10. Ting LL. *Golf ball aerodynamic behaviour as affected by the dimple depth and dimple shape changes*. in Asia-Pacific Congress on Sports Technology. 2005. Tokyo, Japan: Australasian Sports Technology Alliance.
11. Aoki K, Nonaka M, Goto T, Miyamoto M and Sugiura M. *Effect of the dimple structure on the flying characteristics and flow patterns of a golf ball*. in ISEA 5th Engineering of Sport Conference. 2004. Davis, California: International Sports Engineering Association.
12. Kim HC, Nakahashi K, and Kim HJ. *Three-dimensional flow analysis around a cylinder with dimples*. in Asia-Pacific Congress on Sports Technology. 2005. Tokyo, Japan: Australasian Sports Technology Alliance.
13. S. Barber, K. Seo, T. Asai and M.J. Carré. *Investigating the effects of orientation on the flight of a non-spinning soccer ball*, Asia-Pacific Congress on Sports Technology. 2007. Singapore.
14. Carré MJ, Asai T, Akatsuka T and Haake SJ. *The curve kick of a football 2: flight through the air*. Sports Engineering, 2002. **5**: p. 183-192.
15. Barber S, *The aerodynamics of association footballs*, in Mechanical Engineering. 2007, University of Sheffield.
16. Fluent-Incorporated. Fluent 6.2 User's Guide. 2005.
17. Asai T, Takano S, Carré MJ and Haake SJ. *A fundamental study on aerodynamics of soccer ball*. in Proceedings of 83rd Japan Society of Mechanical Engineering Conference (Fluid engineering division). 2005.

List of Figures

Figure 1. General mesh structure.

Figure 2. Balls 1-7 at an orientation of 0° .

Figure 3 C_D vs. Re for Balls 1-3 compared to known data.

Figure 4. Mesh structure most suitable for soccer ball analysis.

Figure 5. Velocity contours taken at a central plane (m/s, side view) and total pressure contours (Pa) for Ball 1, Ball 2 and Ball 3 and the smooth sphere.

Figure 6. Variation of C_S with orientation for Ball 1, Ball 2 and Ball 3, $Re = 1.0 \times 10^6$.

Figure 7. Oil flow visualisation for Ball 1 at 0° at $Re = 1.0 \times 10^6$ (coloured by particle ID).

Figure 8. Shear stress contours (Pa) on the rear of (a) Ball 1, (b) Ball 2 and (c) Ball 3 with separation points marked in black (indicating separation) and red (indicating separation at a seam).

Figure 9. Example of velocity and turbulence intensity contours at various rotational angles.

Figure 10. Radius contours of two balls.

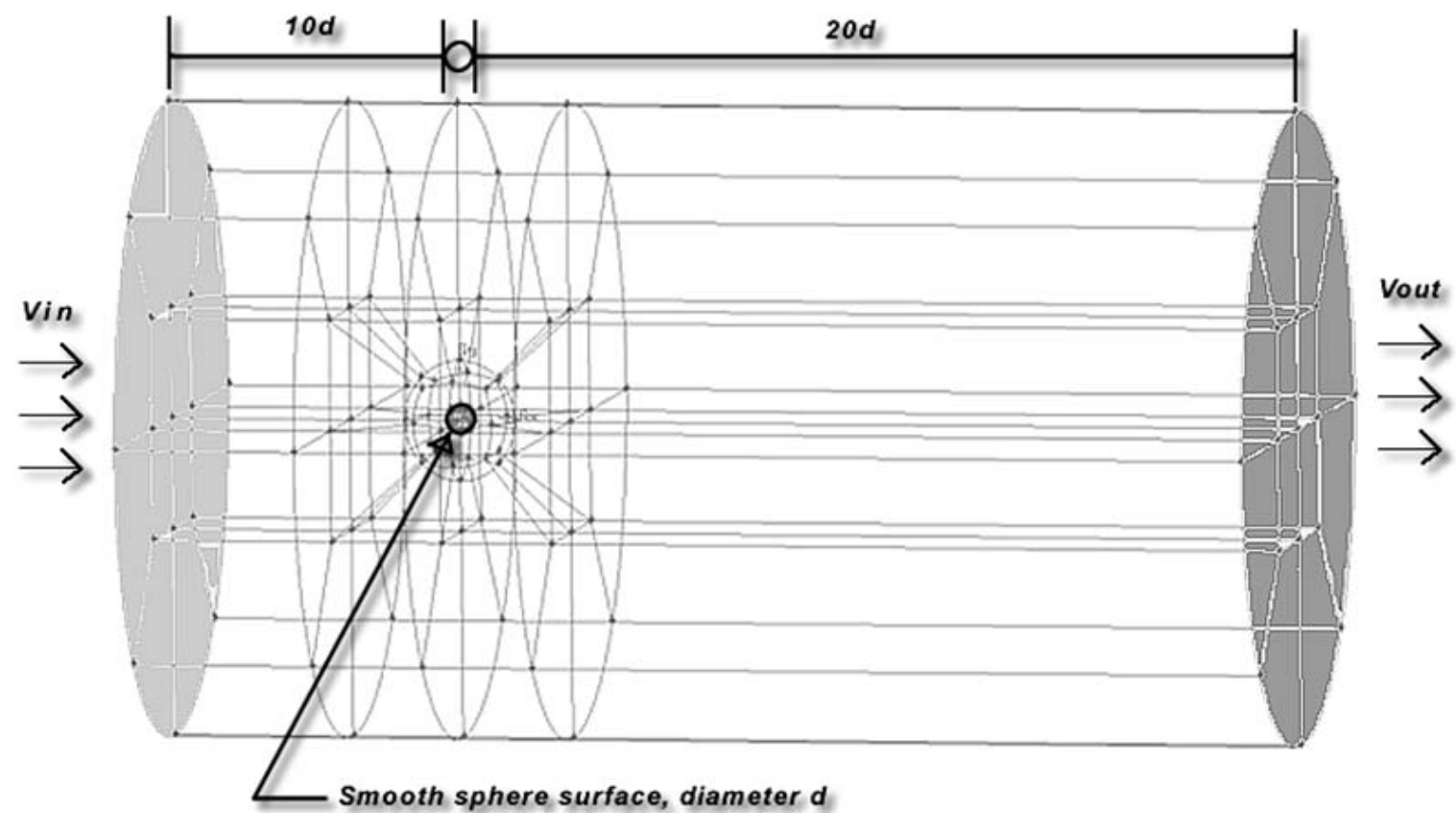
Figure 11. Approximate trajectory of an erratic free-kick.

Figure 12. Predicted trajectories of Balls 1-3 at an initial orientation of 0° .

Tables

Table 1 Summary of C_D results compared to experiment.

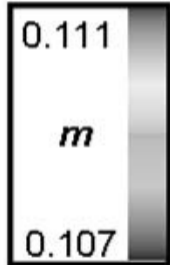
Table 2. Summary of solver details.



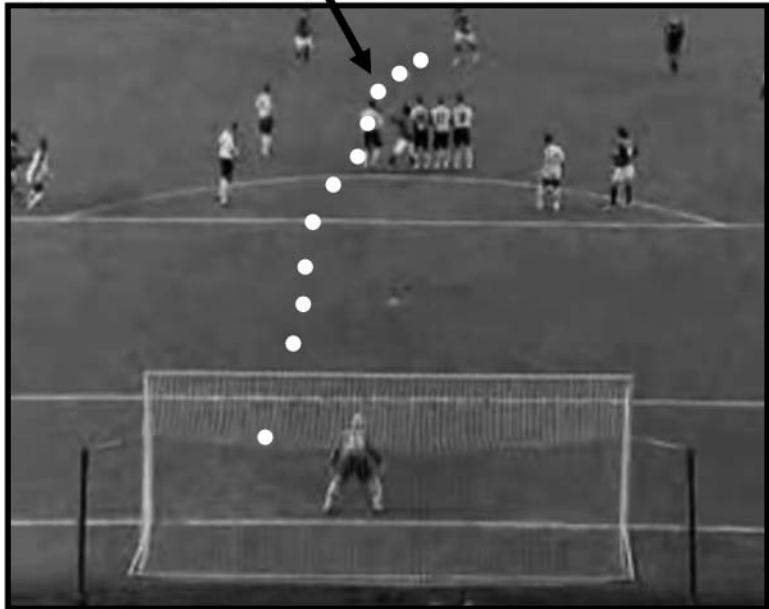
Ball 1



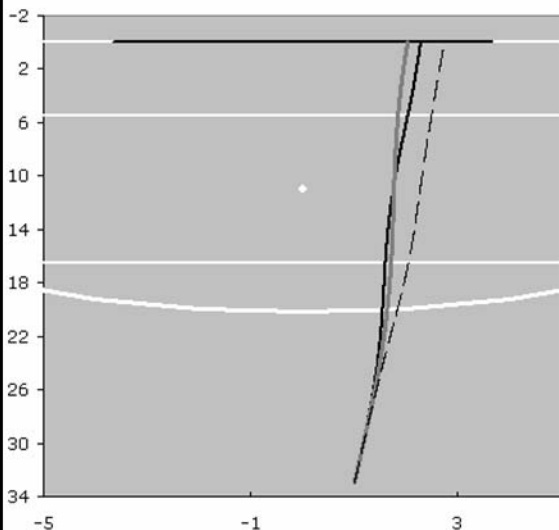
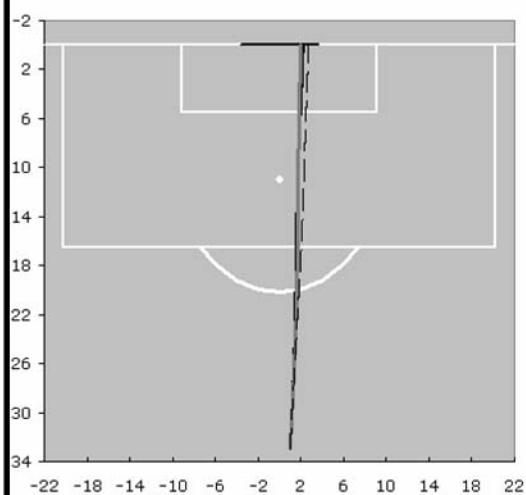
Ball 3



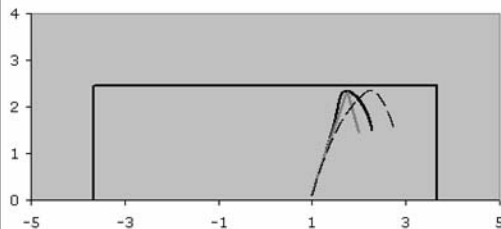
Approximate trajectory



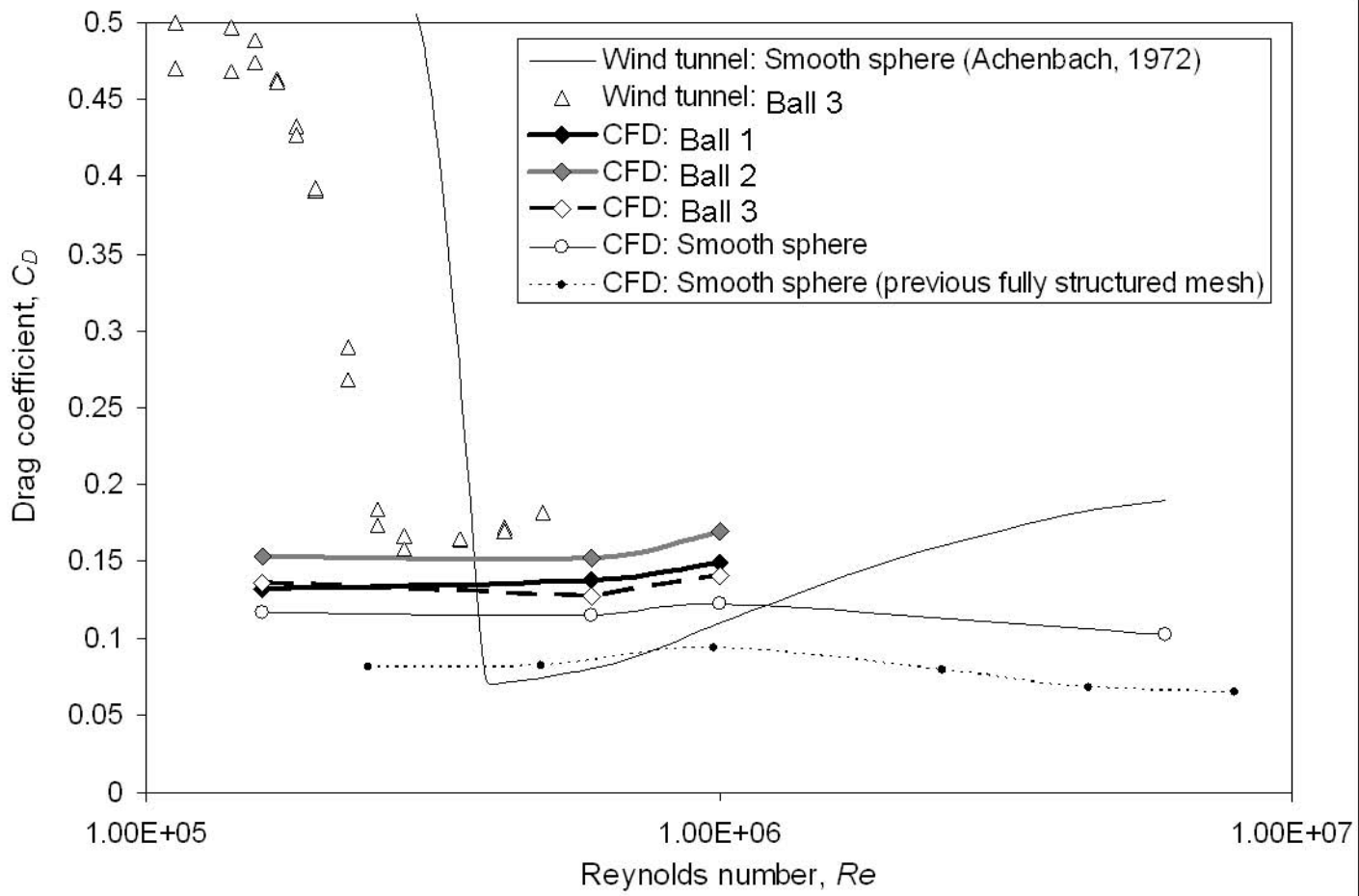
Top View



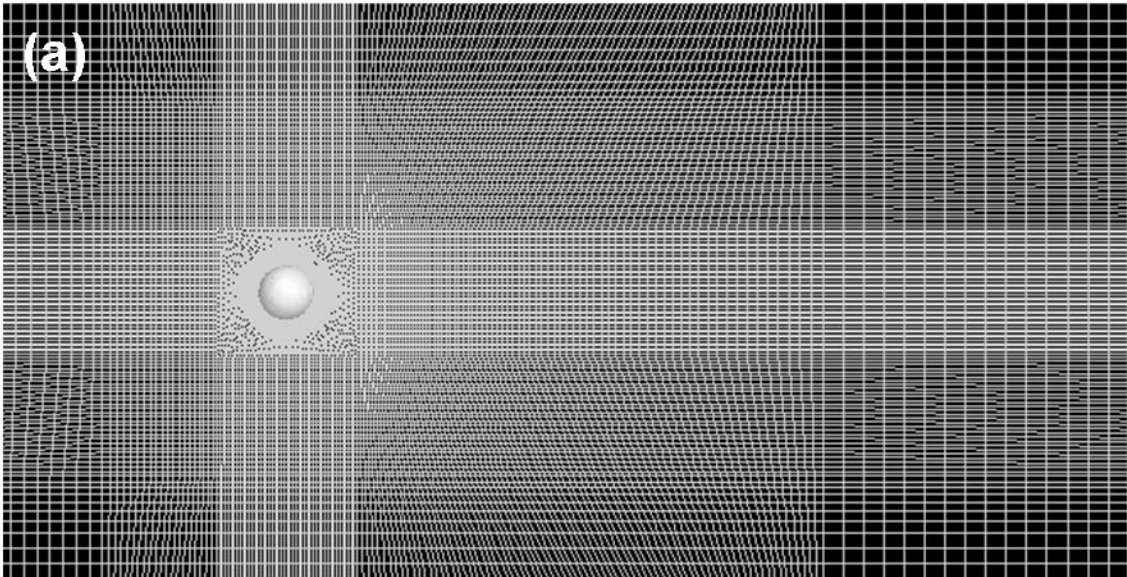
Player View



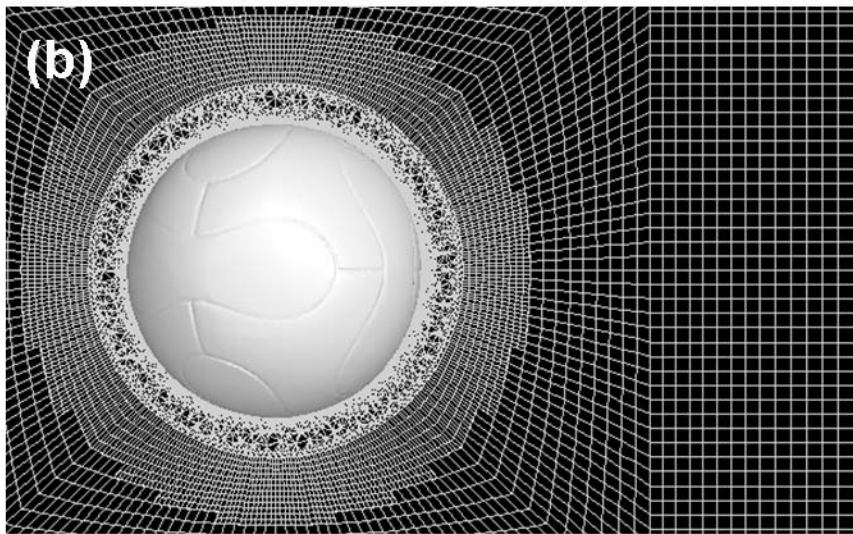
- Ball 1
- - - Ball 2
- Ball 3



(a)



(b)





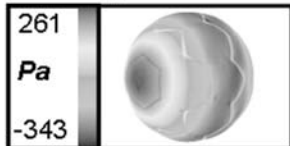
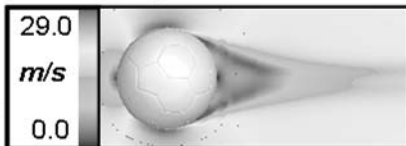
Generic soccer ball
Asai *et al.*, 2005

$$Re = 4.4 \times 10^5$$

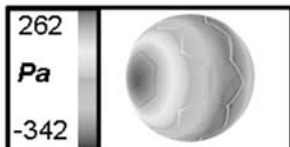
Velocity

Total pressure

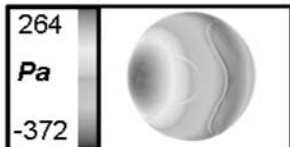
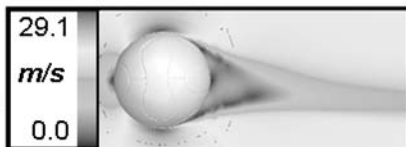
Ball 1
 $Re = 1.0 \times 10^6$



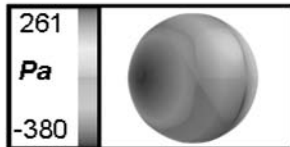
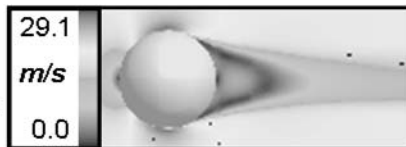
Ball 2
 $Re = 1.6 \times 10^5$

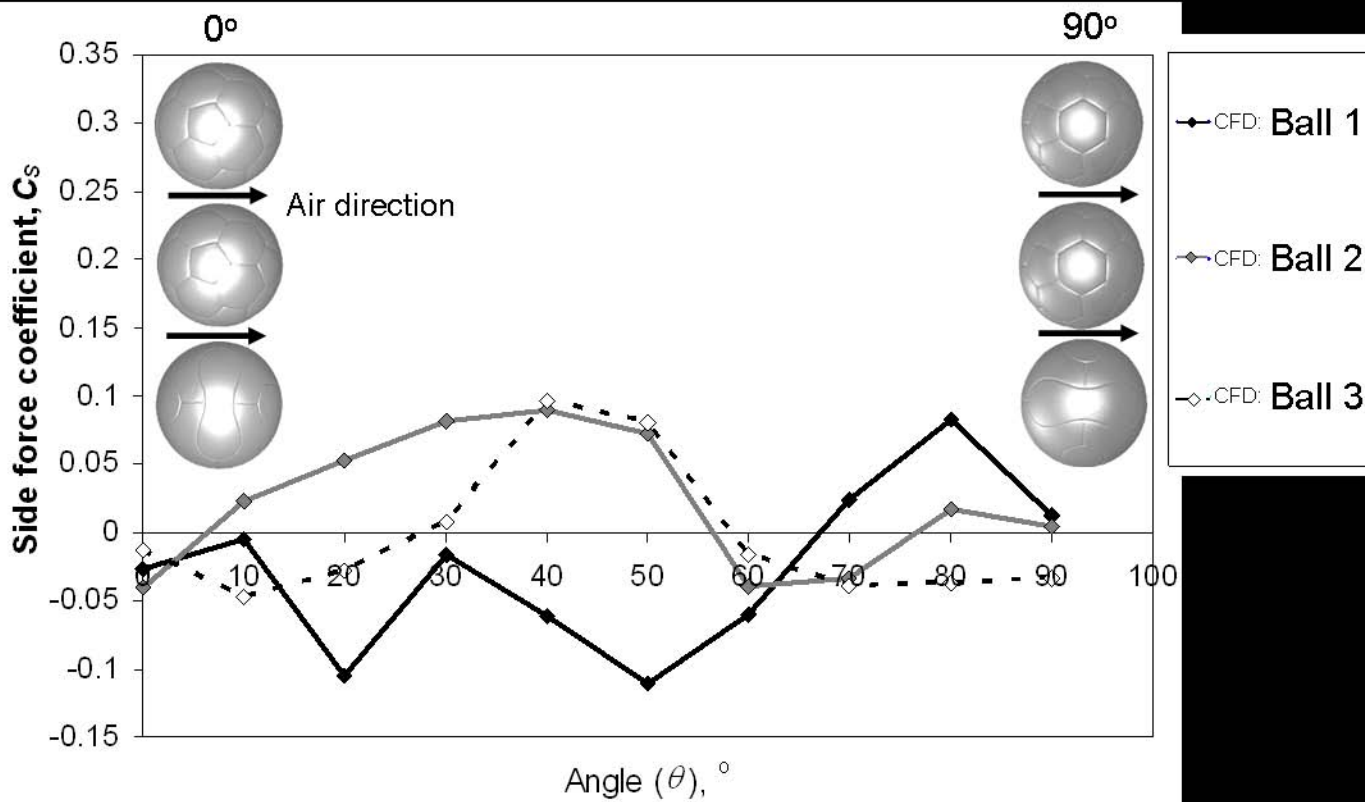


Ball 3
 $Re = 1.0 \times 10^6$



Smooth
 $Re = 1.0 \times 10^6$







FAR SIDE



BOTTOM

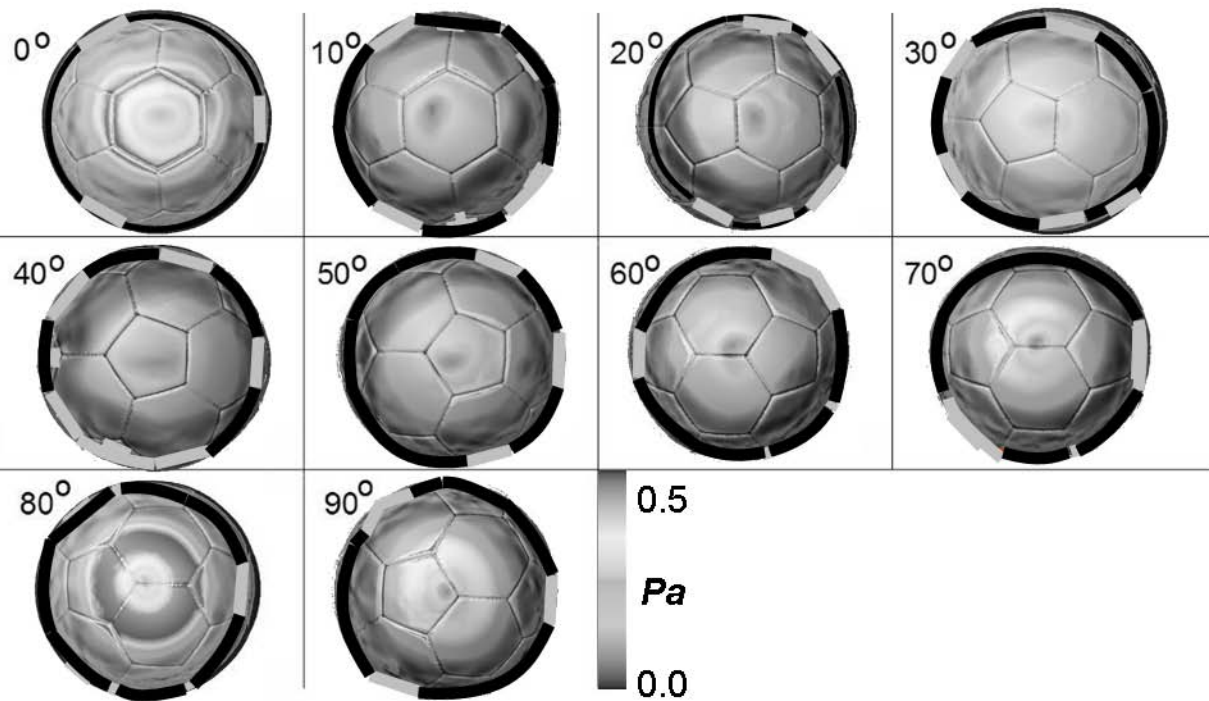


TOP

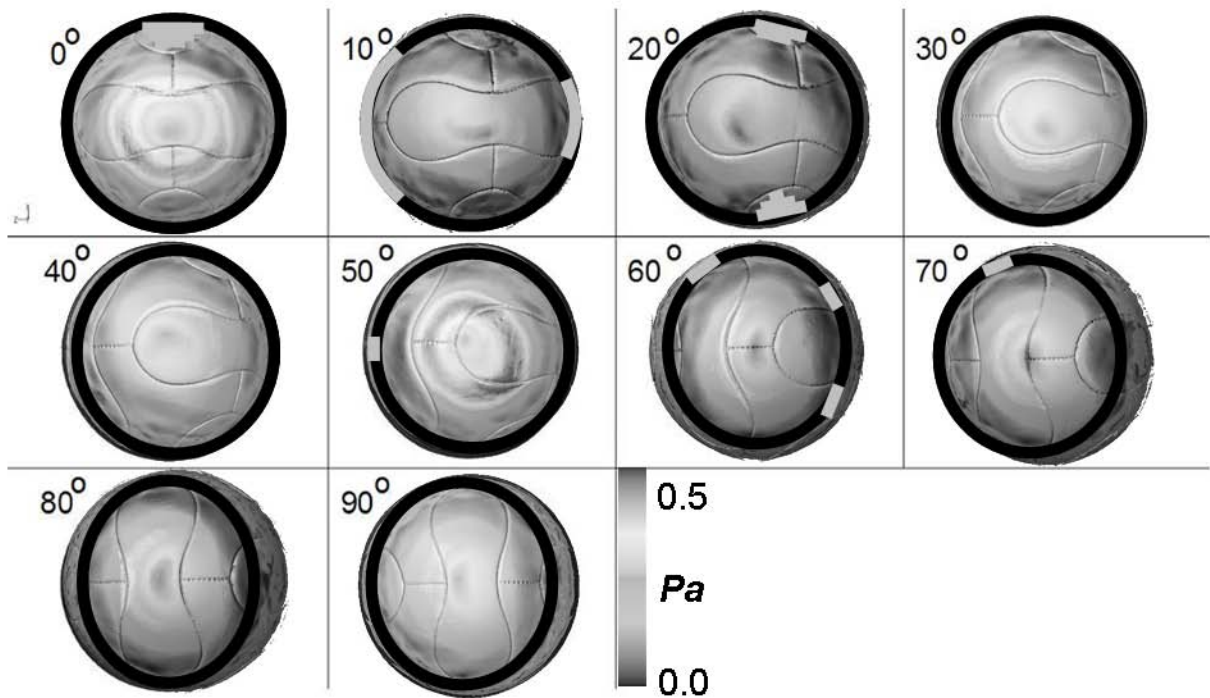


NEAR SIDE

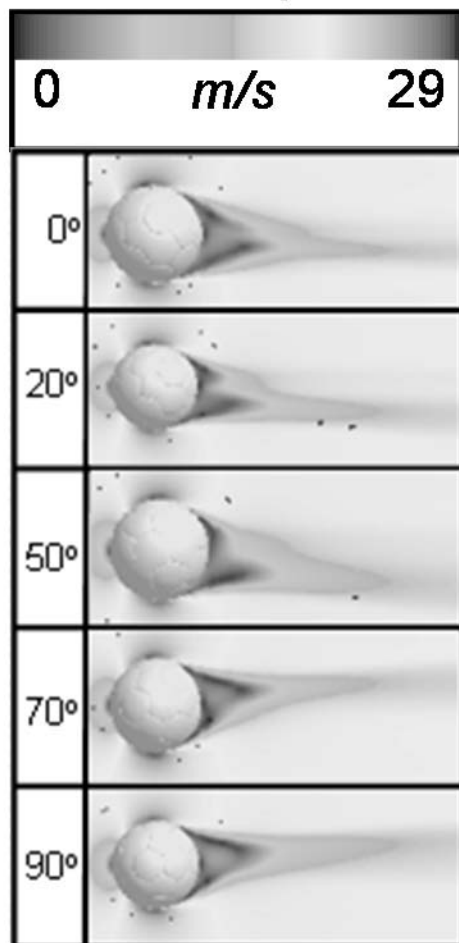
(b) Shear stress contours: Ball 2



(c) Shear stress contours: Ball 3



Velocity



Turbulence intensity

